

A Proton Conductive Coordination Polymer II. Proof of Proton Conduction of Dihydrogen Origin in $[N,N'$ -Bis(2-hydroxyethyl)dithiooxamidatocopper(II)] by Protodes

Seichi Kanda^{*,#} and Fumio Yamamoto

The University of Tokushima, Minami-josanjima, Tokushima 770

(Received July 6, 1995)

An example of proton conduction in a coordination polymer was examined. Dependence of the specific conductivity on hydrogen pressure was quite strong in the title compound with a few types of protodes. The mechanism of electric conduction of this coordination polymer is discussed in connection with related phenomena of the same compound.

The proton conduction through chains of hydrogen bonds and hydrogen absorption through crystal lattice channels in the interior of the solids are of great practical importance, for example, as catalysts for reduction, for hydrogen storage, and for hydrogen gas detection. The theoretical and experimental studies have been done with both organic and inorganic compounds, on which comprehensive reviews, monographs, and accounts were published.^{1–4} One of us has reported examples of copper-containing coordination polymers.^{5–7} In a family of the semiconductive (N,N' -disubstituted dithiooxamidato)coppers, (R_2 dtoaCu), shown in Fig. 1, has only one derivative, the substituents R's of which are HOC_2H_4 , that is protonically conductive as well as electronically conductive. The proton conductivity as a function of vapor pressure of H_2O and D_2O was reported in our last paper,⁶ while in this paper we try to prove the protonic conductivity of the bulk type by showing the effects of dihydrogen pressure and use of several types of protodes composed from Pd.

Experimental

Materials: N,N' -Bis(2-hydroxyethyl)dithiooxamide

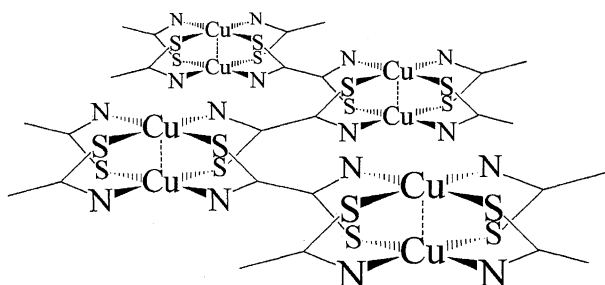


Fig. 1. A probable molecular structure of dithiooxamidatocopper(II). For simplicity the substituents R's on the nitrogen atoms are omitted.

[#]Present address: Kobe Women's Junior College, Minatojima-nakamachi, Chuo-ku, Kobe 650.

(Mallinckrodt Chemical Works) was recrystallized from distilled water (abbreviated as $(HOC_2H_4)_2dtoaH_2$). The coordination copper(II) polymer was prepared as described in our previous paper.⁶ Palladium black was prepared as follows: Aqueous $PdCl_2$ was reduced to a metallic precipitate by formic acid in an alkaline aqueous solution, washed with hot pure water, freed of water in vacuo, and stored. Before use it was activated by hydrogen sorption through polarization in 0.1 M hydrochloric acid (1 M = 1 mol dm^{-3}) on a Pt electrode. Dihydrogen electrolytically obtained from water with a Ni electrode was purified by flowing it through glass tubing with three compartments containing SiO_2 gel, heated Cu wire at 600 °C, and P_2O_5 dispersed on glass fibers at liquid nitrogen temperature, successively. A controlled amount of H_2 gas was introduced into the conductivity cell through evacuated tubing with a needle valve.

Protode and Composite Pellets: Three types of pellet assemblies for conductance measurements were prepared: a 70-mg pellet of the coordination polymer was molded at 30 MPa for one minute in a die ($\phi = 12$ mm) under reduced ambient pressure. The molded pellet, e, was pressed again with Teflon[®] sheets (0.1 mm thick) of parts a and b on both sides at 100 MPa for three minutes as shown in Fig. 2A. Three types of assembly with protodes were examined for the pellets as follows; (1) assembly with single layer type protodes: instead of part b Teflon[®] pieces, portions of 13 mg each of activated palladium powder (2 pieces of c) were put on both sides of the molded pellet e, and the assembly was pressed at 330 MPa for 10 min in a die, (2) Assembly with multilayer type protodes: three layers of mixed compositions were substituted for the above single Pd layers; the activated Pd powder and the coordination polymer, the ratios of which are 1 : 9 (d_1), 5 : 5 (d_2) and 8 : 2 (d_3), were blended. These layers (4 mg for each) are arranged in the order from inside to outside on both side of the pellet. Finally these are pressed under 330 MPa in a die for ten minutes. (3) Spattered-Pd type: this molded pellet e with Teflon[®] sheets a and b, was pressed at 330 MPa instead 100 MPa, and Pd metal was spattered-coated on the pellet covered with Teflon[®] sheets a's on both its sides using an Ion Coater (IB-5 Eiko Engineering Limited). The electrical contact to the spattered Pd was taken through an activated Pd-black powder pellet.

For comparison, a single layer type assembly was prepared using copper fine powder instead of Pd-black.

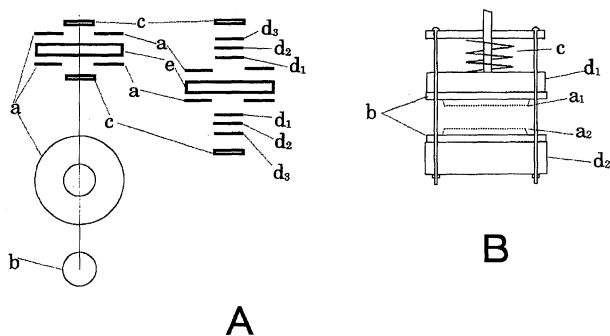


Fig. 2. Assemblies of pellets with protodes (A), and a holder for conductance measurements (B). A: (a) Teflon[®] ring sheets, (b) Teflon[®] circular sheets, used for pre-mold, (c) Pt/Pt pellets of 13 mg weight each, (d) three layers of mixed compositions, 4 mg for each, (e) 70 mg pellet of $(HOC_2H_4)_2dtoaCu$. B: (a) Copper plate electrodes, (b) Teflon[®] block insulators, (c) spring for contacts. See text for details.

Electrical Measurement: Vibrating reed electrometer, Takeda Riken TR 84, and a vacuum conductivity cell were used as before.^{5a,5b,6)} The electrical connection to the assembly 1, 2, or 3 was taken through activated Pd pellets or bored copper plates (Fig. 2B, a_1 , a_2) which were pressed by a spring force of 2 N (Fig. 2B, c) through metal plate d_1 , d_2 , and Teflon[®] plates b's. In advanced of measurements, each pellet assembly was heated to 90 °C under a vacuum to eliminate the effect of water vapor. The resistivity of the blank cell was greater than 10^{15} ohm. Hydrogen was introduced

into the conductivity cell slowly until it reached 2 kPa at room temperature (20 ± 3 °C) to avoid an unfavorable temperature elevation (even burning some times) of the pellet. This might be attributed to a strongly exothermic reaction of absorption of hydrogen into Pd protodes between zero to 2 kPa pressure; the α - β phase transition of Pd- H_x completes at this pressure. Thereafter hydrogen gas was introduced at the prescribed pressures.

Results

Hydrogen Pressure Dependencies of the Electrical Conductivity due to the Type of Protode:

The electrical conductivities of the specimens with the three types of protodes are shown in Figs. 3, 4, and 5, as functions of hydrogen or nitrogen pressures. For comparison, a result where a copper layer of fine powder was used instead of the single layer of activated Pd black, is shown in Fig. 3A (■). As shown in Figs. 3, 4, and 5, the dinitrogen presence with the Pd protodes are ineffective for their conductivities of the specimens, in the pressure range examined (Δ in Figs. 3A, 4A, and 5). The repeated cycles of increase and decrease of hydrogen pressure seem to improve the promptness of response of conductivity for the pressure change in cases of the single- and multi-layer protodes, especially the single layer one. In the case of the single layer protode (type 1) the conductivity increases by a factor of ten from the initial conductivity under vacuum, for the first introduction of H_2 up to 10^4 Pa, but it keeps constant thereafter up to 7×10^4 Pa as shown in Fig. 3.

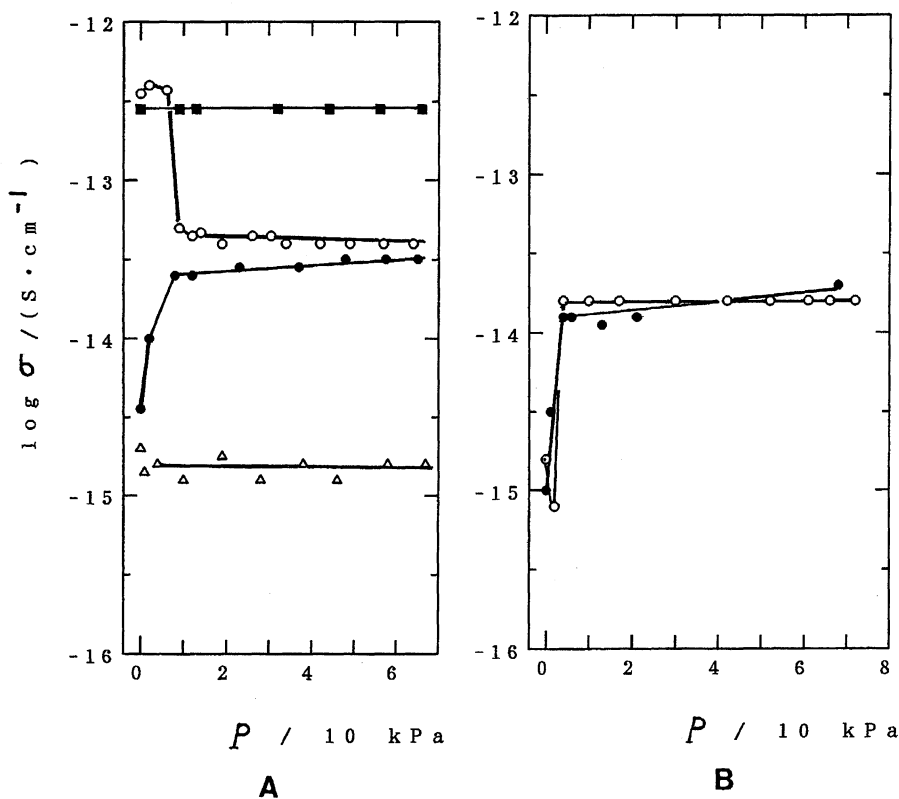


Fig. 3. Conductivity under hydrogen or nitrogen atmosphere, with single type palladium black or copper protode. A: ■: with copper powder electrode in H_2 , ○, ●: palladium black protode in H_2 , △: palladium black protode in N_2 , B: ●, ○: palladium black protode in H_2 , all the measurements were repeated in this order.

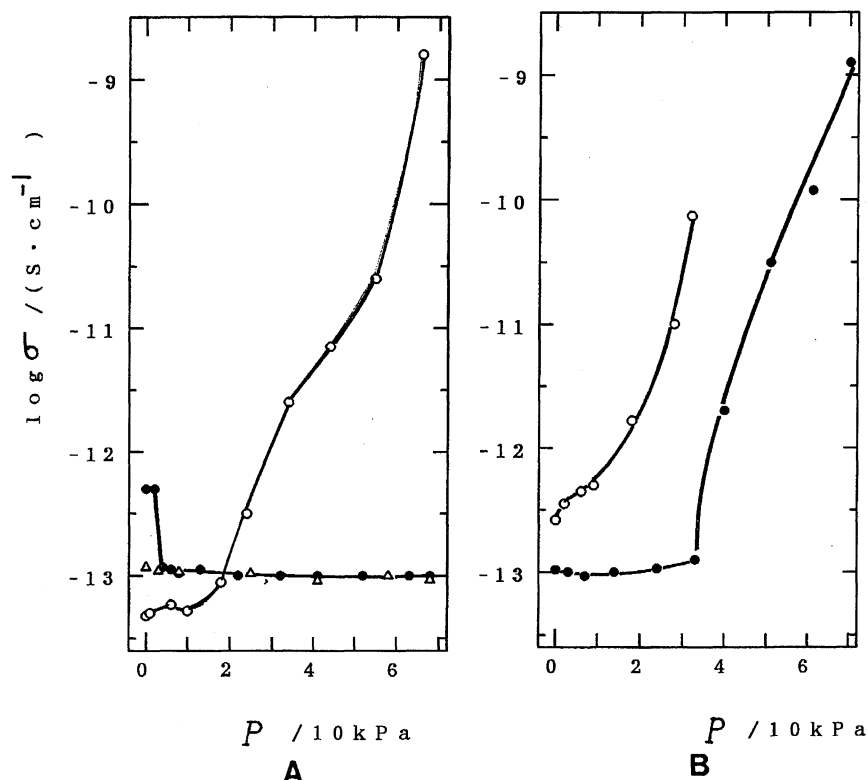


Fig. 4. Conductivity under H_2 or N_2 with the multilayer type protode. A: \bullet , \circ : in H_2 , \triangle : in N_2 , B: \bullet , \circ : in H_2 . The measurements were repeated in this order. The final point \circ in B at 33 kPa is employed in Fig. 7.

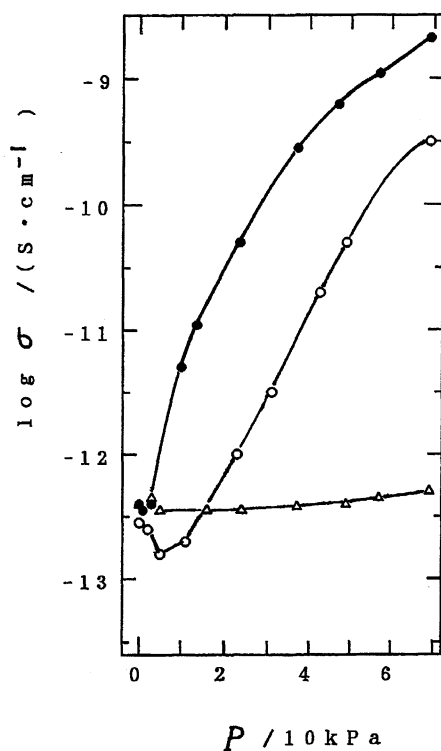


Fig. 5. Conductivity under H_2 or N_2 with spattered Pd protode in the following order. \circ : in H_2 , \triangle : in N_2 , \bullet : in H_2 (employed in Fig. 7).

The multilayer protode (type-2) is more responsive, starting from the second cycle, but thereafter the reproducibility is not perfect (Fig. 4). The quite poor responses in the first cycle in both type-1 and -2 are worth explaining. The spatter-coated electrode (type-3) shows much better reproducibility than the others (Fig. 5). For all three types of electrodes, some drops of the conductivity at the first introduction of H_2 in the first cycle were observed. Pressure reduction by pumping out the H_2 gas results in essentially reversible values of the conductivities, although a rather long waiting time is required to get reliable values.

For the specimens of better responsiveness (type-3), $\log (\sigma / \text{S cm}^{-1})$ was plotted against $\log (P(\text{H}_2) / \text{Pa})$ (Fig. 6). For the relationship

$$\log \sigma = A \log P - B, \quad (1)$$

curve 1 higher than 30 kPa in Fig. 6 gives $A = 5.4 \pm 0.2$, $B = 35.5 \pm 1.1$; curve 2 lower than 25 kPa gives $A = 3.1 \pm 0.1$, $B = -23.7 \pm 0.5$, for the ascending path in the pressure range shown. In the lower pressure region, about 20 min for each plot is required to reach stable conductivity values, but in the higher region the stable values were reached quickly. At lower than 20 kPa ($\log P / \text{Pa} = 4.3$) the conductivity has durable drifts which makes it difficult to obtain reproducible values for theoretical consideration, especially in its pressure descending path as shown (--- in Fig. 6). The conductivity of each pellet with type-3 protode at zero pressure was reproducible even after repeated runs, but the zero-pressure

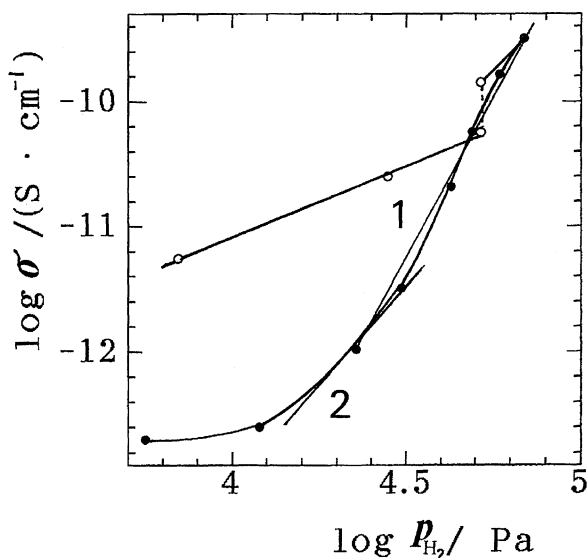


Fig. 6. $\log \sigma$ against $\log P$ with the spattered-Pd electrode in the pressure ascending (●) and descending (○) orders. ○ ---- ○ reveals the waiting time of 13.5 h. To obtain the other two descending points, the waiting are 10 to 20 min.

conductivities with type-1 and -2 protodes are hardly reproduced on their pressure cycles.

Temperature Dependence of the Conductivity at a Certain Pressure of H_2 : Conductivity was measured as a function of temperature under isobaric conditions for three types of electrode: copper electrode, spatter coating Pd protode (type 3) backed up with activated Pd, and the multilayer protode (type 2). The pressures of ambient gases were 24 kPa of N_2 with copper electrode, 25 and 69 kPa of H_2 with type-3 protode, and 33 kPa of H_2 with type-2 protode, respectively. As shown in Fig. 7, at temperatures higher than 60 °C, the three pellets have almost the same behavior. The extrapolated three lines to the lower temperature side focused to an intersection. The activation energies in lower temperature ranges are for hydrogen and type 3 electrodes E (25 kPa)=0.63±0.1 eV, E (69 kPa)=2.03±0.1 eV, for hydrogen and type 2 electrodes E (33 kPa)=1.4 eV, and for nitrogen and copper electrodes E (24 kPa)=0.93±0.1 eV.^{8,9)}

Voltage Dependence of Isothermal Conductivity at a Certain Pressure of Hydrogen: At the highest H_2 pressure (70 kPa) the conductivity of type 3 assembly was measured as a function of the electric field strength ($V \text{ cm}^{-1}$). As was shown in a log-log plot in Fig. 8, the Ohm's law region and the square-law (Child's law) region can be noticed by a transition field strength V_x . At a field strength indicated as V_{TFL} the electric current started to increase on time. Therefore the V_{TFL} is shown by an arrow in Fig. 8. Farther voltage application was stopped to avoid damage to the assembly.

If the space-charge limit and the trap-filled limit are applicable formally to these two voltages from the ordinary simplified theory,^{1,8)} charge carrier concentration n_o and trap concentration n_t are obtained as follows, where ϵ_0 and ϵ (=31.6) are the permittivity of the vacuum and of the specimen respectively, q and L are the protonic charge and the

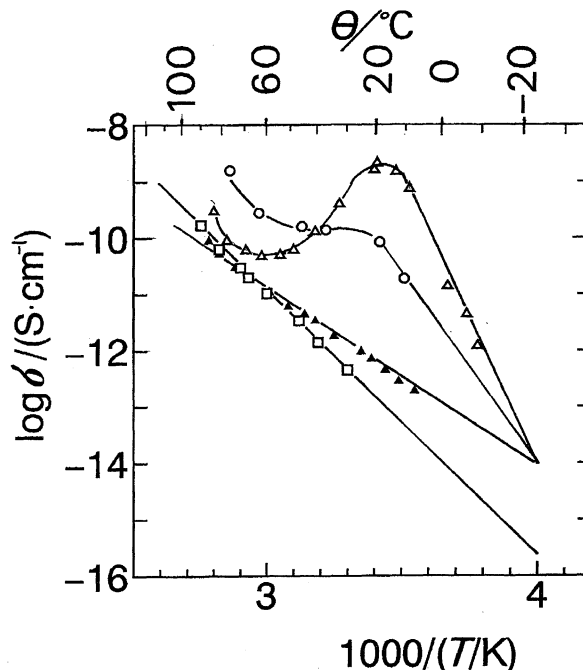


Fig. 7. Temperature dependence of the conductivity at isobaric conditions of H_2 for the spattered Pd and the multilayer protode, and of N_2 for Cu electrode. □: Cu (24 kPa), ▲, △: the spattered protode (25, 69 kPa), ○: the multilayer protode (33 kPa).

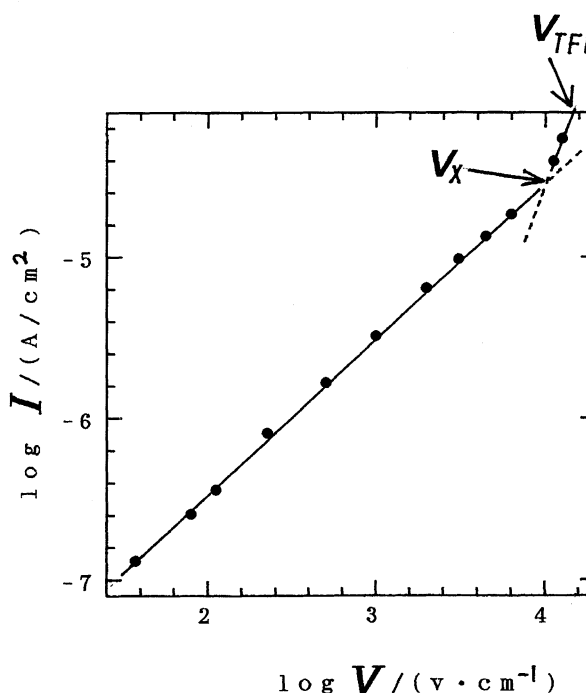


Fig. 8. Field strength dependence of isothermal conductivity at 70 kPa of H_2 with the spattered protode. V_x and V_{TFL} are that of the Ohmic-Child transition and that of trap-filled limit (see text).

pellet thickness, and V'_x and V'_{TFL} are applied voltages on the specimen:

$$n_o = 2\varepsilon_0\varepsilon V'_x/(qL^2) = n_H = 8.2 \times 10^{12} \text{ cm}^{-3}, \quad (2)$$

$$\text{and } n_t = 2\varepsilon_0\varepsilon V'_{\text{TFL}}/(qL^2) = n_- = 1.3 \times 10^{13} \text{ cm}^{-3}. \quad (3)$$

The proton mobility, μ_H , is also evaluated as $4.5 \times 10^{-3} \text{ cm}^2 \text{ V}^{-1} \text{ S}^{-1}$.

Discussion

Molecular Structure: The very strong antiferromagnetic interaction between Cu^{2+} 's and the semiconductivity in the homologous series of (*N,N'*-disubstituted dithio-oxamidato)copper(II)'s and a few diffuse X-ray diffraction peaks suggest that these compounds are essentially amorphous polymers owing to the random coordinations of S and N around Cu^{2+} ion pairs. An example of the most probable molecular structure is shown in Fig. 1. The idea of this two-dimensional structure was also supported from surface flow patterns of the Langmuir–Blodgett film drawn on the water surface.⁷⁾

Proton Conduction: In comparison with each other the results shown in Figs. 3, 4, and 5, the following hypotheses or recognition based on the experimental facts are proposed: (1) The electrical conductivity is composed of an electronic part and a protonic constituent, which is attributed to protonic activity in the specimen as was discussed in our previous paper.⁶⁾ (2) Dinitrogen does not contribute to increase in the proton activity in the specimen naturally, but the conductivity under N_2 atmosphere is that due to electrons in the semiconductive specimen that have not been in contact with dihydrogen. These results are essentially reproducible. (3) Although differences in the degree of their perfection are noticed between the cases with the protodes of the three types, an increase in ambient dihydrogen pressure raises the protonic conductivity in the coordination polymer through these protodes. (4) The maximum specific conductivities at the ambient temperature (ca. 20 °C) for each case of the three types of protodes under the highest H_2 pressure examined, 70 kPa, were 4×10^{-14} , 1.6×10^{-9} , and $2 \times 10^{-9} \text{ S cm}^{-1}$ for types 1, 2, and 3 respectively. (5) Concerning the prompt responsiveness of conductivity to the H_2 pressure change and the reproducibility for H_2 pressure cycle (0–70 kPa), the type-3 protode seems to be the best, followed by type-2 and -1 in this order as were seen above. Pd crystal expands in volume, as a solid–solid (α – β) transformation, by absorbing hydrogen. This causes macroscopic strain at the interface between the protodes and the specimen; the thicker the protode pellets are the more the strain is. Thickness is about 20 nm for type 3, and about 0.5 mm for types 1 and 2. The effects of thickness can be the origin of a wide variety of the responsiveness and reproducibility of the conductivity for the pellets with the protodes 1, 2 or 3. The α – β transformation of Pd crystals at 20 °C occurs under 10 kPa, and can be the reason for the abrupt drops and the poor reproducibility of conductivities under the relatively low pressure shown in Figs. 3 and 4.

On the basis of the preceding five hypotheses, the H_2 pressure dependency of conductivity at constant temperature (Figs. 3, 4, and 5), the temperature dependencies of the

conductivity at the constant pressures (Fig. 7) and the voltage dependence of conductivity (Fig. 8) must be discussed even if only qualitatively. Generally speaking the possible factors deciding apparent conductivity in the values, both at equilibrium and at the transient processes, seems to be (1) the absorption rate of proton into Pd metal, (2) the rate of transmission (permeation) of protons from the positive protode to the specimen and from the specimen to the negative protode, and any other structure-sensitive boundary surface phenomena, or (3) the drift-mobility and number of protons in the coordination polymer. Absorption and desorption rates of hydrogen into and from palladium metal are not small enough to explain these large irreversibilities. Real electric current for measurements ($< 10^{-10} \text{ amp}$) are too small to make any change of real H^+ amount in the type-3 protode ($> 10^{-4} \text{ coulomb}$, 10^{-9} mol) as a proton source of charge carrier. Therefore the (1)-factor could be excluded as a rate-determining factor. If the (2)-factor is the rate-determining step, the resulting conductivity may not be such highly sensitive to $P(\text{H}_2)$. As the result, if the (3)-factor could be sensitive to $P(\text{H}_2)$, (3) must be rate-determining in this $P(\text{H}_2)$ -sensitive conduction process.

The number of free protons and/or the proton bridge or chain generated along the two-dimensional network of the copper coordination polymer⁵⁾ appears to be most important in the observed complex phenomena, that is, in the irreversibility and nonreproducibility, shown in Figs. 3, 4, and 5. As mentioned before, the poor response of conductivities in the type-1 assembly at higher than 10 kPa (Fig. 3) suggest that the proton injection to the specimen from the expanded Pd peace became limited because of the space gap between the Pd powder particles and the specimen after the phase transition. This difficulty was partially overcome by the type-2 (the multilayers) protodes as shown in Fig. 4. That is, the factor-(2) can explain the poor responses in Fig. 3 in a negative way, and explain the better response later than the second cycle in Fig. 4. Protons can be successively injected through the improved contacts even at higher pressure than 10 kPa, and create more ample hydrogen bridge paths in the molecular network even though the reproducibility on increase and decrease of hydrogen pressure was not perfect. As the result, the factor-(3) become rate-determining and $P(\text{H}_2)$ dependent in the better response in the second cycle (○ in Fig. 4A), and also the poor reproducibility in descending path (pressure decreasing, ○ in Fig. 6). The initial creation (● in Fig. 4A) and interruption (○ in Fig. 6) of the proton jump path in the polymer networks are restricted, possibly by geometrical conditions that are hard to control. In the type-3 assembly the close contacts of Pd with the polymer pellet were not harmed by the hydrogen absorption, because the geometrical deformation of the thin-spattered palladium film was too small to cause space gaps between the protodes and the polymer.

The intersection of extrapolated lines at certain temperature ($T=250 \text{ K}$) in Fig. 7 means the following relation of activation energy in lower and higher temperature ranges:

$$\begin{aligned}
 E \text{ (low temp. } \triangle \text{ high } H^+) \\
 &= 2.0 \text{ eV} > E \text{ (high temp. } \blacktriangle \text{ low } H^+) \\
 &= 0.6 \text{ eV.}
 \end{aligned}
 \quad (4)$$

On the contrary, in the cases of doping of various vapors into intrinsic semiconductors, the following relationship has been established, which is valid for electronic conductors:^{8,9)}

$$\begin{aligned}
 E \text{ (intr.; higher temperature)} \\
 &> E \text{ (extr.; lower temperature).}
 \end{aligned}
 \quad (5)$$

As we have assumed a priori, H_2 is not a simple dopant for this semiconductive coordination polymer, but is a source of a new charge carrier, the proton. As the activation energy of protons is larger than that of electrons the above relationship (4) is reasonable. That is, the proton conduction began to be predominant below 60 °C and at 69 kPa of $P(H_2)$.

As was discussed in our previous paper, the most probable molecular structure of this compound is a two dimensional conjugate d- π electron network consisting of C, N, S, and Cu, and HOC_2H_5 - substituents on the nitrogen atoms, terminal protons of which form hydrogen bonds to adjacent ligands. This secondary system, the intermolecular hydrogen bond system, is characteristic of the substituent, which is absent in the several other homologues.⁵⁾ This system might behave as a charge transfer system cooperating with the d- π and π - π conjugate primary system, and also as a proton transport system independently from the primary conjugate π electronic system. The idea of semiconductive primary system proposed first from direct conductivity measurements⁵⁾ was supported by electrochemical technique using a platinum electrode/dithiooxamidatocopper and its homologues.¹⁰⁻¹²⁾

Coupled e^- - H^+ transport in a Flavonoid Functionalized membrane was measured in aqueous buffer solution as a model of liposomal membranes.¹³⁾ The electronic and ionic conductivity of poly(4-methylpyrrole-3-carboxylic acid) was analyzed in terms of a two-phase model composed of electrolyte solution and the polymer, using twin electrode voltammetry and impedance spectroscopy.¹⁴⁾ Imidazole was investigated and it was established that the charge carrier is a proton in its crystallographic c -direction, that of the hydrogen-bonding chain.¹⁵⁾ In the path in the solid phase, the molecular reorientation followed by discharge at the negative electrode is the rate-determining step, but in its liquid state, the thermal generation and transport of charge is the step.¹⁵⁾ In poly(benzimidazole), $2 \times 10^{-4} \text{ S cm}^{-1}$ and $8 \times 10^{-4} \text{ S cm}^{-1}$ were obtained as conductivities under pretreatment at a humidity of 0 and 100% respectively using Pd-black protodes without exposing the polymer film to gaseous hydrogen.¹⁶⁾ In $H_2O_2PO_2 \cdot 4H_2O$, a very rapid proton conductor, conductivity of $4 \times 10^{-3} \text{ S cm}^{-1}$ was obtained at room temperature using Pd-black protodes fixed into glass sections that divided the two compartment of a cell. The compartments were filled with a solution that was in contact with the sample.¹⁷⁾ Here also, no hydrogen gas was used as the proton source during the conductivity measurements.

In our data, the conductivity was strongly dependent on the

ambient hydrogen pressure, the determinant factor of which seems to be the situation of the copper coordination polymer at room temperature rather than the Pd electrode.

Behavior of Dihydrogen on the Surface and Inside of the Assembly: On the surface of the Pt electrodes, the homolytic splitting of hydrogen molecules has been recognized as the standard process. The neutral atom is then ionized to a proton and an electron, and these thermally diffuse in the crystal lattice, or drift under the influence of an electric field. From the positive electrode (protode), protons drift into the coordination polymer and move to the negative protode, but from the negative electrode, electrons are injected into the conduction band of the polymers and drift to the positive protode.

As mentioned previously,¹⁻⁴⁾ a number of transition metal hydrides have been synthesized, which are classified as ionic, metallic, and covalent. In those cases hydrogen is regarded as a negatively charged species even partially, that is hydrido complexes. In this study, not only the palladium protodes but also the copper coordination compound was exposed directly to hydrogen gas molecules. Although most of the copper hydrido complexes, either binary or more complex, have been prepared and isolated not by direct reaction with H_2 but with other reductants, the identification of hydrido-copper bonds as intermediates in many cases had been discussed since the wide studies of Halpern in aqueous solution.¹⁸⁾ Recently a few copper hydride compounds were isolated in the solid state by direct reaction with H_2 , obtaining $Cu_3(H_2)$ and $Cu_3H_2(H_2)_2$.¹⁹⁾ Our recent works on the reaction of H_2 with copper coordination polymers or discrete ammine complexes also suggest the probable existence of copper hydrido species as intermediates.²⁰⁻²²⁾ From this information, we pay attention to the probable formation of $Cu-H^-$ species in this circumstance. For the realization of $Cu-H^-$, two possible routes can be proposed; in the first place the heterolytic splitting of H_2 molecule on the surface of the copper complex compound, and secondly reduction of protons originated in any way by electrons that meet in the copper complex. In both processes protons compose the interligands hydrogen bonds or free charge carriers, and H^- 's coordinate to copper ions. The hydrido complex formation and the hydrogen bond formation seem to be cooperative actions. Although spectroscopic detection of $Cu-H^-$ bond formation has not succeeded so far, the possibility of the hydrido formation is worth pursuing. This point seems to be concerned closely with the $P(H_2)$ - σ relations discussed above, where the conductivity, σ , is proportional to about the 5th power of $P(H_2)$. As is well known, σ is proportional to the product of mobility μ and carrier concentration n_o , now $n(H^+)$. Probably $n(H^+)$ is proportional to $P(H_2)$, so that μ must be proportional to the 4th power of $P(H_2)$. The variable proton-jumping distance between the H^+ site to site on the two-dimensional network could cause this high sensitivity of μ .

Conclusion. Use was made of a method of controlling the hydrogen pressure, giving farther direct evidence of proton transfer through the specimen. The response of conductivity is quite sensitive to hydrogen pressure, and this

would imply that hydrogen gas reacts directly with the coordination polymer either on the surface or the bulk, at least at room temperatures.

References

- 1) L. Glasser, *Chem. Rev.*, **75**, 21 (1975).
 - 2) R. G. Linford and S. Hackwood, *Chem. Rev.*, **81**, 327 (1981).
 - 3) M. A. Ratner, *Acc. Chem. Res.*, **15**, 360 (1982).
 - 4) H. D. Carstanjen, *Z. Phys. Chem. (Neue Forge)*, **165**, 141 (1989).
 - 5) a) S. Kanda, K. Ito, and T. Nogaito, *J. Polym. Sci., Part C*, **17**, 151 (1967); b) S. Kanda, *Nippon Kagaku Zasshi (J. Chem. Soc. Jpn., pure chem. sec.)*, **83**, 560 (1962); c) S. Kanda and S. Kawaguchi, *J. Chem. Phys.*, **34**, 1070 (1961); d) S. Kanda and Y. Saito, *Bull. Chem. Soc. Jpn.*, **30**, 192 (1957).
 - 6) S. Kanda, K. Yamashita, and K. Ohkawa, *Bull. Chem. Soc. Jpn.*, **52**, 3296 (1979).
 - 7) K. Ohkawa, F. Morita, and S. Kanda, *Nippon Kagaku Kaishi, Kagaku to Kogyokagaku*, **1983**, 910.
 - 8) A. Rose, *Phys. Rev.*, **97**, 1538 (1955).
 - 9) B. Mallik, A. Gosh, and T. N. Misra, *Bull. Chem. Soc. Jpn.*, **52**, 2091 (1979).
 - 10) L. M. Abrantes, L. M. Castillo, M. Fleischmann, I. R. Hill, L. M. Peter, G. Mengoli, and G. Zotti, *J. Electroanal. Chem.*, **177**, 129 (1984).
 - 11) G. Zotti, G. Mengoli, and F. Decker, *Mol. Cryst. Liq. Cryst.*, **121**, 337 (1985).
 - 12) F. Decker, M. Fracastoro-Decker, G. Zotti, and G. Mengoli, *Electrochem. Acta*, **30**, 1147 (1985).
 - 13) Y. Kobuke and I. Hamachi, *J. Chem. Soc., Chem. Commun.*, **1989**, 1300.
 - 14) X. Ren and P. G. Pickup, *J. Electrochem. Soc.*, **139**, 2097 (1992).
 - 15) A. Kawada, A. R. McGhie, and M. M. Labes, *J. Chem. Phys.*, **52**, 3121 (1970).
 - 16) D. Hoel and E. Grunward, *J. Chem. Phys.*, **81**, 2136 (1977).
 - 17) M. G. Shulton and A. T. Howe, *Mater. Res. Bull.*, **12**, 701 (1977).
 - 18) J. Halpern, "Annual Review of Phys. Chem., 1965," Annual Reviews, Palo Alto, CA (1965), p. 103.
 - 19) G. J. Kubas, *Acc. Chem. Res.*, **21**, 120 (1988); Ref. 39; R. H. Hauge, Z. H. Kafafi, and J. L. Margrave, "The Physics and Chemistry of Small Clusters," Richmond, VA (1986).
 - 20) S. Kanda and N. Munemori, *J. Electroanal. Chem.*, **274**, 281 (1989).
 - 21) S. Kanda, N. Mizobuchi, and R. Sioda, *J. Electroanal. Chem.*, **375**, 243 (1994).
 - 22) S. Kanda, T. Kori, and S. Kida, *J. Solid State Chem.*, **108**, 299 (1994).
-